International Journal of Computer Assisted Radiology and Surgery (2018) 13:797–804
https://doi.org/10.1007/s11548-018-1757-z

ORIGINAL ARTICLE

Experimental validation of robot-assisted cardiovascular catheterization: model-based versus model-free control

Xiaomei Wang[1] · Kit-Hang Lee[1] · Denny K. C. Fu[1] · Ziyang Dong[1] · Kui Wang[1] · Ge Fang[1] · Su-Lin Lee[2] · Alex P. W. Lee[3] · Ka-Wai Kwok[1]

Received: 31 January 2018 / Accepted: 26 March 2018 / Published online: 2 April 2018

Abstract

Purpose In cardiac electrophysiology, a long and flexible catheter is delivered to a cardiac chamber for the treatment of arrhythmias. Although several robot-assisted platforms have been commercialized, the disorientation in tele-operation is still not well solved. We propose a validation platform for robot-assisted cardiac EP catheterization, integrating a customized MR Safe robot, a standard clinically used EP catheter, and a human–robot interface. Both model-based and model-free control methods are implemented in the platform for quantitative evaluation and comparison.

Methods The model-based and model-free control methods were validated by subject test (ten participants), in which the subjects have to perform a simulated radiofrequency ablation task using both methods. A virtual endoscopic view of the catheter is also provided to enhance hand-to-eye coordination. Assessment indices for targeting accuracy and efficiency were acquired for the evaluation.

Results (1) Accuracy: The average distance measured from catheter tip to the closest lesion target during ablation of model-free method was 19.1% shorter than that of model-based control. (2) Efficiency: The model-free control reduced the total missed targets by 35.8% and the maximum continuously missed targets by 46.2%, both indices corresponded to a low p value (≤ 0.05).

Conclusion The model-free method performed better in terms of both accuracy and efficiency, indicating the model-free control could adapt to soft interaction with environment, as compared with the model-based control that does not consider contacts.

Keywords Cardiac electrophysiology · Robotic catheterization · Model-based control · Model-free control · Endoscopic view · MR Safe

Introduction

Catheterization is an interventional procedure for the treatment of cardiovascular diseases. In cardiac electrophysiology (EP) for atrial fibrillation, a long (1.5-m) and flexible EP catheter is inserted from femoral vein to heart chamber, e.g., left atrium (LA), to obtain an electro-anatomical map (EAM) [1], then to create lesion inside the chamber using radio frequency (RF) ablation. The non-conductive scars created by ablation, usually on the ostia of the pulmonary veins, will isolate abnormal EP signals to treat heart rhythm disorders (arrhythmias) [2]. This minimally invasive procedure requires delicate and consistent motion of the catheter tip via the manipulation on the catheter handle. However, even provided with X-ray visual guidance, maneuvering of the distal tip to the desired location is still a challenging task in manual catheterization procedures.

To facilitate precise manipulation, robotic catheterization has attracted much attention. Despite the advent of several commercial robotic catheter systems, such as Sensei^{TM}X (Hansen Medical, Inc., Mountain View, CA, USA), Niobe (Stereotaxis, Inc., St. Louis, MO, USA) and Armigo^{TM} Remote Catheter System (Catheter Precision, Inc., Mount

✉ Ka-Wai Kwok
kwokkw@hku.hk

1 The Department of Mechanical Engineering, The University of Hong Kong, Pokfulam, Hong Kong

2 The Department of Computing, Imperial College London, London, UK

3 Prince of Wales Hospital, The Chinese University of Hong Kong, Shatin, Hong Kong

Olive, NJ, USA) [3], currently, there is not any study on MRI-guided tele-manipulation of the catheter. The conventional navigation relies on intra-op X-ray to provide a real-time navigation interface [4]. Compared with X-ray, intra-op MRI could offer superior details and differentiate soft tissues [5], which makes it a better choice for cardiac EP catheterization. MRI-guided EP procedure has been validated by several research groups with patient trials [6,7], which have shown its wide potential in clinical use. However, there is neither commercial product nor research prototype of an MRI-guided robotic system for EP catheterization. In this paper, we would like to integrate our customized MR Safe robotic platform [8] with a human-robot control interface to evaluate the control performance of model-based and model-free methods, as well as how they influence the hand-to-eye coordination of operator. Another advantage of MRI-guided catheterization is the superior accuracy of MR-based tracking [9,10], in which catheter position could be measured under the same coordinate as imaging, eliminating potential registration error. This characteristic also allows the generation of a virtual endoscopic view from the catheter tip. The hand-to-eye coordination can hence be simplified, as the operator can control the catheter movement in the endoscopic view instead of conventional Cartesian space. Such an endoscopic visual guidance could improve accuracy and potentially reduce perforation risk in a simulated ablation task [11].

Traditional robotic control is based on the kinematic/dynamic model of the robot configuration and motion [12]. The distal bendable section of a catheter could be modeled as a continuum robot. Constant curvature (CC) approach is one of the most common methods for kinematic modeling of continuum structures [12]. CC models of catheters [13,14] have simple formulations that facilitate implementation. Catheter deflection could also be predicted from actuation force using quasi-static force deflection models based on beam theory [15]. Other approaches also include modeling the bendable sections as discretized rigid links with passive spherical joints, which has been demonstrated in 2D motion planning simulation [16]. However, external disturbance to the catheter, such as the pulsatile blood flow and contact with the cardiac chamber, can promptly deteriorate the reliability of these models in real-life applications. Furthermore, the accuracy of these kinematic/dynamic models strongly depends on proper selection of the structural parameters, but the search for these coefficients is often a heuristic process.

In contrast, model-free control methods avoid complicated system identification procedures for specific analytical models. The control mapping is solely sensory data. A PID controller for hybrid control of a 4-tendon catheter has been proposed in [17], where the actuation commands rely only on real-time position/force error feedback. Another representative model-free controller for a catheter prototype has been proposed in [18], which bases on real-time estimation of the Jacobian that relates sensory feedback at the catheter tip and the actuator command. Although these model-free approaches demonstrate promising control performance, they were validated with custom-made catheter prototypes that are not employed in current clinical practice. Therefore, the performance of model-based and model-free control methods in tele-operated robotic catheterization system still need further validation.

In this paper, we focus on the validation of the proposed experimental setup with human–robot interface. A control mapping for hand-to-eye coordination is implemented based on the virtual endoscopic view. Quantitative indices are designed to evaluate the performances of model-based and model-free methods on a static left atrial ablation task. The model-based controller is designed based on the constant curvature kinematic model [13,14]. The model-free controller utilizes position feedback to update the kinematic Jacobian [19]. Experimental evaluations were carried out using a standard clinically used catheter, which was tele-manipulated via an MR Safe robotic actuator (Fig. 1) under a virtual endoscopic guidance (Fig. 2). The major contributions are listed below:

1. Control mapping for hand-to-eye coordination based on the virtual endoscopic view utilizing model-based and model-free control methods ("Control methodology" section);
2. Experimental validation platform for tele-operated robotic EP catheterization using a customized MR Safe robotic actuator ("Experimental setup" section);
3. Performance evaluation and comparison of model-based and model-free control methods on a simulated ablation task carried out by ten subjects ("Controller performance evaluations" section).

Control methodology

Catheter robot control

A customized catheter robot [8] was used to replace manual control of the bi-directional EP catheter as shown in Fig. 1. Both MR-conditional catheter and standard clinically used EP catheters are compatible to this robot. The robot enables manipulation of three degrees of freedom (DoFs) for bending, rotation and insertion of the catheter. The details of the catheter model are introduced in " Model-based control" section.

Generation of endoscopic view

As shown in Fig. 2a, a virtual camera view (endoscopic view) is defined and attached to the catheter tip, of which the z-axis is aligned along the tip normal axis. The pose of

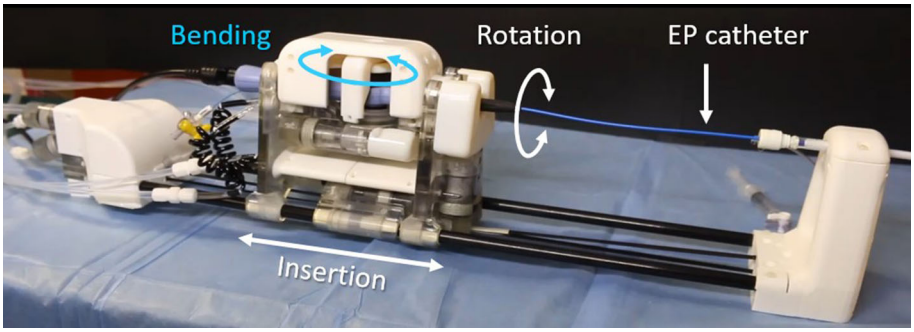

Fig. 1 Customized MR Safe robotic catheter manipulator providing the 3-DoF manipulation (bending, rotation and insertion) of a standard clinically used EP catheter

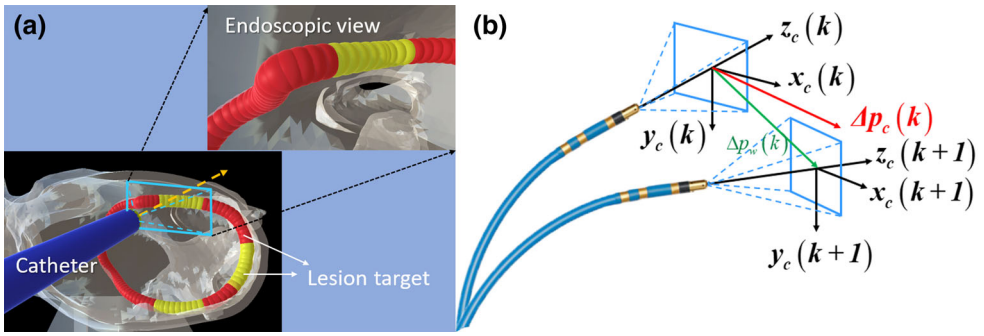

Fig. 2 **a** Left atrial EP roadmap showing the virtual lesion targets defined close to the pulmonary vein ostia: yellow for ablated regions; red for incomplete ones. The virtual endoscopic view is rendered from the catheter tip point of view. **b** Schematic diagram showing the movement of the catheter tip at time step k and step $(k+1)$, along with its endoscopic image plane

the endoscopic frame could be sampled by the tracking system available in MRI-guided catheterization. In this work, we propose to correlate the catheter motion in endoscopic view with users input motion. First, the transformation of the tip position from the Cartesian space to the $X-Y$ coordinates with respect to (w.r.t) the 2D endoscopic view has to be derived. Incremental movement of the virtual camera at the catheter tip is denoted by $\Delta \boldsymbol{p}_w = \left[\Delta x_w \ \Delta y_w \ \Delta z_w\right]^{\mathrm{T}}$ w.r.t the world coordinate (Cartesian space) $\{\boldsymbol{W}\}$, while this movement w.r.t. the endoscopic coordinate $\{\boldsymbol{C}\}$ is denoted as $\Delta \boldsymbol{p}_c = \left[\Delta x_c \ \Delta y_c \ \Delta z_c\right]^{\mathrm{T}}$ (Fig. 2b). Δz_c is the unit vector that aligns along the catheter tip normal orientation.

To ensure the consistency of the steering direction of the catheter tip, the rolling of the camera along its z-axis is fixed during the transition. The rolling axis is defined by a unit vector $\boldsymbol{z}_c \in \Re^3$. Thereby, the x- and y-axis of the camera frame, also act as the horizontal and vertical axes $\left[\Delta x_c \ \Delta y_c\right]^{\mathrm{T}}$ of its image plane. The 3×3 rotation matrix ${}^{C}_{W}\boldsymbol{R} = \left[\boldsymbol{x}_c \ \boldsymbol{y}_c \ \boldsymbol{z}_c\right]^{\mathrm{T}}$ from the world $\{\boldsymbol{W}\}$ to camera $\{\boldsymbol{C}\}$ coordinate frame can be formed. Skipping the last row, the matrix becomes ${}^{C}_{W}\widehat{\boldsymbol{R}} = \left[\boldsymbol{x}_c \ \boldsymbol{y}_c\right]^{\mathrm{T}}$ with dimension of $\Re^{2\times 3}$, which transforms the tip displacement relative to its image plane coordinate, i.e., $\Delta \boldsymbol{p}_c = {}^{C}_{W}\boldsymbol{R}\left(\Delta \boldsymbol{p}_w\right)$.

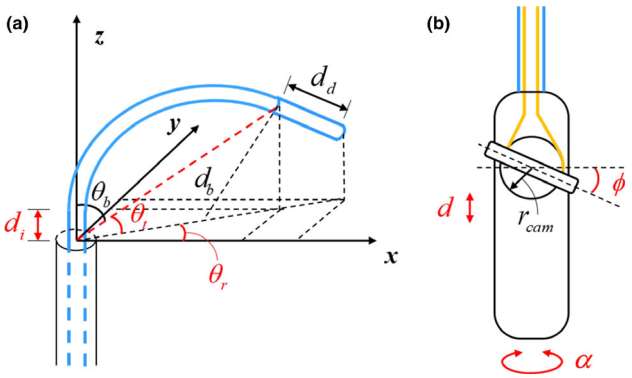

Fig. 3 Schematic diagram of a typical catheter mechanism. **a** Constant curvature geometry of the distal section of the catheter. **b** Geometry of steering knob on the catheter handle indicated with its insertion distance d, twisting angle ϕ, and rotating angle α

Model-based control

Model-based methods rely on the pre-established kinematic/dynamic model of the flexible catheter. Regarding the catheter distal section as a continuum robot, constant curvature model [13,14], beam model [15], n-rigid links model [16] were investigated in the previous work. Standard clinically used steerable catheters could bend in two directions in the same plane by pulling tendons. The for-

ward kinematic model of the clinically used catheter based on D-H parameters has been established in [13]. This model is based on two assumptions, which are constant curvature and zero torsion. The equivalent model is briefly presented in Fig. 3.

As shown in Fig. 3a, the catheter distal section has 3 DoFs: the axial translation denoted by d_i, the bending angle denoted by θ_b, the rotation angle denoted by θ_r. The movements of the catheter are driven by manipulating the catheter handle as shown in Fig. 3b, where d, α and ϕ represent the insertion distance, the twisting angle of the knob and the rotation angle of the handle, respectively.

The axial translation d_i of the catheter is approximately equal to the insertion distance of the handle d ($d \approx d_i$). The relation between the rotating angle of handle α and tip θ_r is given as $\theta_\mathrm{r} = K\alpha$. The parameter K represents the torsional transmission effectiveness, which is taken as 1 in our experiment because of the low-friction between the catheter body and polytetrafluoroethylene (PTFE) pipeline. Based on constant curvature assumption, the bending motion of the catheter tip is related to the knob twisting angle ϕ by

$$\Delta R\,(\pi - 2\theta_t) = r_\mathrm{cam}\phi\,(1+k) \tag{1}$$

where $\theta_t = \pi/2 - \theta_\mathrm{b}$, ΔR is the radius difference between inner and outer arcs of the bendable section, r_cam is the radius of the cam fixed with steering knob and k is the backlash factor to account for the tension-free wire displacement [14], which can be taken as 1 when both pull wires are well tensioned.

Based on the coordinate system in Fig. 3, the position of end effector (catheter tip) can be calculated as below using d, ϕ and α

$$\boldsymbol{p} = \begin{bmatrix} \mathrm{c}\,(K\alpha)\left(\frac{L}{M\phi}\mathrm{s}^2\,(M\phi) + d_d s\,(2M\phi)\right) \\ s\,(K\alpha)\left(\frac{L}{M\phi}\mathrm{s}^2\,(M\phi) + d_d s\,(2M\phi)\right) \\ d + \frac{L}{2M\phi}s\,(2M\phi) + d_d c\,(2M\phi) \end{bmatrix} \tag{2}$$

where $M = \frac{r_\mathrm{cam}(1+k)}{\Delta R}$, d_d is the length of the rigid distal section, and L is the length of the bending part of the catheter. The symbol $\mathrm{s}(\cdot)$ and $\mathrm{c}(\cdot)$ are $\sin(\cdot)$ and $\cos(\cdot)$ respectively. The original and additional bending curve lengths are L_b and ΔL, respectively. As ΔL is small compared to L_b, it could be ignored, that is

$$L = L_\mathrm{b} + \Delta L = L_\mathrm{b} + 2r_\mathrm{cam}\theta_t \approx L_\mathrm{b} \tag{3}$$

This catheter robotic manipulator can be described by a function of input variables relative to actuator $\boldsymbol{q} = \begin{bmatrix}\phi & \alpha & d\end{bmatrix}^\mathrm{T}$ and the position of the catheter tip in the frame of camera view $\{\boldsymbol{C}\}$ is denoted as $\boldsymbol{p}_c = \begin{bmatrix}x_c & y_c & z_c\end{bmatrix}^\mathrm{T}$. The corresponding differential function could be represented as

$$\dot{\boldsymbol{p}}_c = \boldsymbol{J}\dot{\boldsymbol{q}} \tag{4}$$

where the Jacobian matrix $\boldsymbol{J}$ could be calculated by differentiating the catheter tip position $\boldsymbol{p}_w$ with respect to the input variable $\boldsymbol{q}$. $\boldsymbol{p}_c$ and $\boldsymbol{p}_w$ could be transformed using the rotation matrix ${}^C_W\boldsymbol{R}$.

With the Jacobian matrix of forward kinematics, we could establish its inverse kinematic function $\dot{\boldsymbol{q}} = \boldsymbol{J}^{-1}\dot{\boldsymbol{p}}_c$, which can be discretized to

$$\Delta\boldsymbol{q} = \boldsymbol{J}^{-1}\Delta\boldsymbol{p}_c \tag{5}$$

As this goal is to make the catheter tip motion and input motion synchronized, $\Delta\boldsymbol{p}_c$ could be designed as the input read from the 3D motion input device, which is known in each step, and the inverse Jacobian matrix $\boldsymbol{J}^{-1}$ could be calculated using the values in the last time step. With these two factors, the values of actuator variables $\Delta\boldsymbol{q}$ could be obtained.

Model-free control

The model-free control method implemented here is inspired by the optimal control method used in [19], but without the need of force sensor feedback. The Jacobian matrix is obtained and updated by the real-time data collected during the operation. After a quick initialization of the Jacobian matrix, the operator could control the robot with an updating mapping scheme. The main flow of this control is shown as below.

1. Initialization of Jacobian matrix

The 3 DoFs of the actuator for rotation, bending and insertion are independent to each other; therefore, the initialization could be achieved by actuating the three motors in order with an incremental amount Δq_i, $i = 1, 2, 3$, and measuring their corresponding displacements $\Delta\boldsymbol{p}_{ci}$. Then the initial Jacobian matrix could be constructed as $\boldsymbol{J} = \begin{bmatrix}\boldsymbol{J}_1 & \boldsymbol{J}_2 & \boldsymbol{J}_3\end{bmatrix}$, where $\boldsymbol{J}_i = \Delta\boldsymbol{p}_{ci}/\Delta q_i$. A weighting matrix $\boldsymbol{W}$ is designed as $\boldsymbol{W} = \mathrm{diag}\,(\|\boldsymbol{J}_1\|, \|\boldsymbol{J}_2\|, \|\boldsymbol{J}_3\|)$. Therefore, the kinematic function (4) could be represented as

$$\dot{\boldsymbol{p}}_c = \widehat{\boldsymbol{J}}\boldsymbol{W}\dot{\boldsymbol{q}}, \quad \widehat{\boldsymbol{J}} = \boldsymbol{J}\boldsymbol{W}^{-1} \tag{6}$$

which could be discretized as

$$\Delta\boldsymbol{p}_c = \widehat{J}\boldsymbol{W}\Delta\boldsymbol{q} \tag{7}$$

2. Updating of Jacobian matrix

The online update relies on continuous estimation of the Jacobian, which is estimated by solving the following quadratic programming problem:

$$\begin{aligned} &\text{minimize } \left\|\Delta\widehat{\boldsymbol{J}}(k)\right\| \\ &\text{subjectto } \Delta\boldsymbol{p}_c(k) = \widehat{\boldsymbol{J}}(k+1)\,\boldsymbol{W}\Delta\boldsymbol{q}(k), \\ &\qquad \widehat{\boldsymbol{J}}(k+1) = \widehat{\boldsymbol{J}}(k) + \Delta\widehat{\boldsymbol{J}}(k) \end{aligned} \tag{8}$$

where $\Delta\widehat{\boldsymbol{J}}(k)$ is the variable to be optimized, $\widehat{\boldsymbol{J}}(k)$ is the Jacobian matrix at time k, $\widehat{\boldsymbol{J}}(k+1)$ is the new Jacobian estimate at time $k+1$, and $\left\{\Delta\boldsymbol{p}_c(k), \Delta\boldsymbol{q}(k)\right\}$ are displacements in camera view and output of actuator between the last time k and the present time $k+1$. We minimize the Frobenius norm (L_2-norm) of $\Delta\widehat{\boldsymbol{J}}(k)$ for smooth transition of the column vectors of the Jacobian. After obtaining the latest Jacobian, the command to actuators could be calculated by

$$\Delta\boldsymbol{q}(k+1) = \left(\widehat{\boldsymbol{J}}(k+1)\,\boldsymbol{W}\right)^{-1}\Delta\boldsymbol{p}_c{}^*(k+1) \tag{9}$$

where $\Delta\boldsymbol{p}_c{}^*(k+1)$ is the desired motion in camera view.

Experimental setup

MR-compatible robotic catheter platform

We implemented the above-mentioned control algorithms on a customized MR-compatible catheter robot (Fig. 1) [8]. This robot features a master–slave hydraulic transmission that can fully manipulate a standard clinically used catheter with 3 DoFs. Each master unit is actuated by an electric DC motor located in the control room. The actuation energy is then delivered to the slave unit via the long hydraulic transmission pipelines ($\approx$ 10 m). Such design separates the source of energy from the MRI scanner, ensuring negligible EM interference to the MR images. The robot can provide sufficient workspace to perform RF ablation for pulmonary vein isolation as shown in [8].

Left atrial model

The 3D phantom model of left atrium (LA) (Fig. 4a) was obtained from an MRI scan and 3D-printed with soft material (AgliusClear, Stratasys Inc.). The shore hardness of the material is A30-35 and the polymerized density is 1.14–1.15 g/cm^3. The model comprises more than 5000 meshed, which is accurate and glossy enough to reproduce the geometry of real tissues.

To conduct RF ablation inside LA, catheter is inserted at femoral vein, through the inferior vena cava to the right atrium. After puncturing the atrial septum, it reaches LA for RF ablation [20]. In our experiment, a sheath (PTFE pipeline) is placed to form the pathway, guiding the catheter toward the LA phantom with similar entering direction and position to cardiovascular interventions.

Position tracking system

In the experiments, an electromagnetic (EM) tracking system (Aurora V3, Northern Digital Inc.) (Fig. 4a) is utilized to obtain the position and orientation of the catheter tip in world coordinate. This system allows the simultaneous tracking of multiple miniaturized sensor coils in five or six DoFs with sub-degree and sub-millimeter accuracy. In clinical practice, the MRI pulse tracking sequence design [21] can provide the MR-based active tracking system with high-frequency (40 Hz) update.

Robot control interface

The position and orientation of atrial phantom is registered to the Unity 3D environment before the test. The soft LA phantom was fixed on a rigid 3D-printed pedestal, on which six points were predefined for registration between EM coordinate and virtual environment. Once the transformation of reference points was established, the virtual LA in the interface could be registered to 3D-printed LA phan-

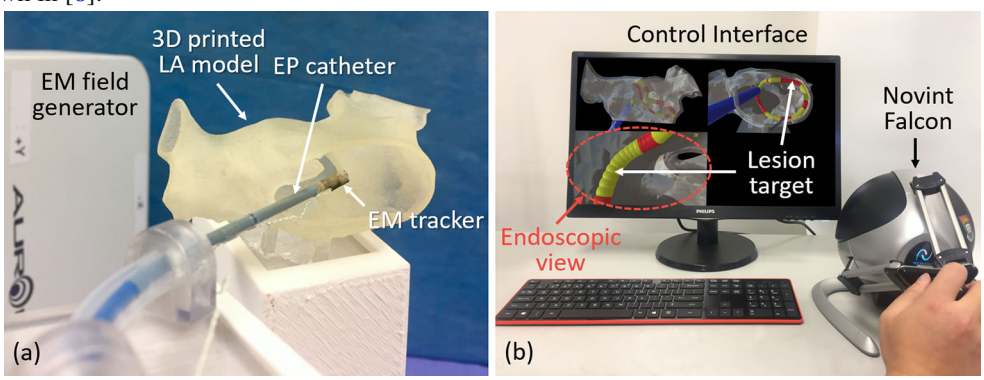

Fig. 4 Experimental setup: **a** left atrial phantom model and the EP ablation catheter. **b** Robot control interface providing the operator with simulated cardiac roadmap displayed in three different camera perspectives, including the virtual endoscopic view

tom. As described in "Position tracking system" section, one 6-DoFs EM tracker (Aurora #610029, Northern Digital Inc.) is attached to the distal end of the catheter, to capture the position and orientation. Hence, the relative geometric configuration between LA phantom and catheter could be measured in real time for visualization and evaluation.

The human–robot control interface provides three virtual sub-views (Fig. 4b), which includes two overall views from different visual angles and one endoscopic view, and all these three sub-views are available to the subjects during the subject test. The overall views can visualize the interaction between the inner cavity environment and catheter tip from the exterior position. The generation of endoscopic view (Fig. 2a) is introduced in "Generation of endoscopic view" section.

The operator can control the catheter tip motion through a 3D haptic device (Novint Falcon haptics controller). An intuitive control can be achieved as the operator could readily perceive the spatial position using the endoscopic view while maneuvering the catheter tip inside the heart chamber. The input motion could be mapped to movement in endoscopic view, instead of Cartesian space, facilitating a more consistent hand-to-eye coordination.

Controller performance evaluations

Simulated ablation task

In our navigation interface, a 3D roadmap of "lesion" targets (in red) composed by 121 spheres reveal around the pulmonary vein ostium on the virtual LA model. The lesion targets are registered to the 3D-printed LA phantom together with its virtual model as mentioned in "Robot control interface" section. The lesion targets are consistently aligned with the LA phantom, since the highly compliant catheter only imposed limited deformation (≤ 2 mm) on the LA phantom and even less on the "lesion" targets. This deformation caused by the catheter tip was insignificant to the resultant accuracy evaluation. When valid ablation (ablation duration and tip-to-target distance are satisfied) performs on the lesion targets, the color of target will turn yellow gradually, representing the corresponding section is successfully ablated. Experimental data, including (1) time, (2) 3D position of the catheter tip, (3) distances from the tip to all of the lesion targets, (4) status of ablation ON/OFF, and (5) ablation status of lesion target represented by values 0–50, are recorded at 20 Hz for offline analysis.

Ten subjects (age ranging from 20 to 30, 7 men and 3 women) were invited to participate in this experimental validation. As a within-subjects design, all the subjects performed both catheter control methods, but in random order. This design can effectively reduce the error variance associated with individual differences, as each subject serves as his/her own standard of comparison [22]. The subjects have technical background but no experience in electrophysiology (EP) procedures. Before the test, cardiac EP catheterization surgery and the manipulation method of the experimental setup were introduced. Each of the subjects was required to perform RF ablation on predefined lesion targets within 3 minutes.

Results and discussion

Accuracy and efficiency are of upmost importance to the clinical practice, which are defined for assessment in the task (Fig. 5). The accuracy could be assessed in terms of (1) the proximity distance measured from catheter tip to lesion target during the ablation, (2) number of times that ablation had been turned on, and (3) average ablation duration; and efficiency could be evaluated by (1) the missed proportion of lesion target segments and (2) the maximum number of continuously missed lesion targets, and (3) the total travel distance of the catheter tip (Fig. 6).

Table 1 shows the performance evaluation result of the subject test, where model-based and model-free control methods in robotic catheterization are compared for each index. Here, the improvement percentage is calculated by

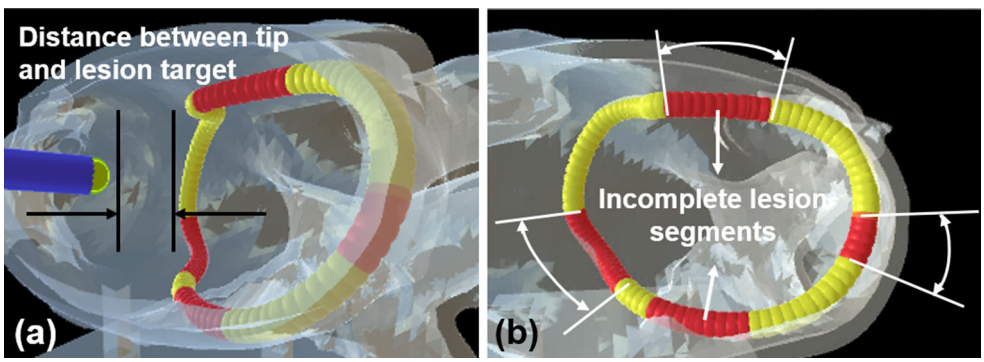

Fig. 5 Two major performance indices, namely accuracy and efficiency defined based on **a** proximity distance measured from tip to lesion target around the pulmonary vein ostia and **b** total length of incomplete lesion segments (red)

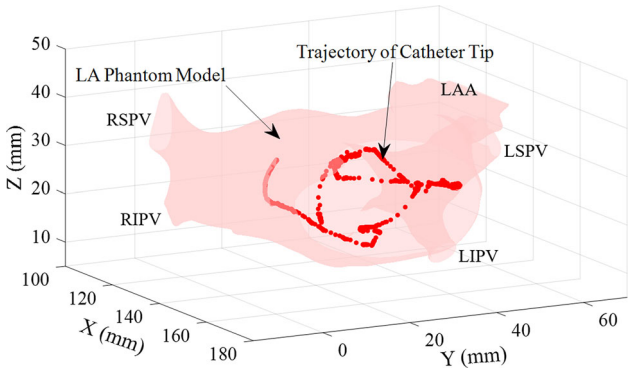

Fig. 6 Trajectory of the catheter tip in the LA phantom model

the increment of model-free method referring to the model-based method.

(a) Accuracy
The average distance between catheter tip to the closest lesion target during ablation of the model-free control method was 19.1% shorter than that of the model-based one, indicating the advantage of the model-free control to approach the static target. The Model-based method had fewer times of ablation turned on and shorter ablation duration. The better accuracy of the model-free control can be interpreted that the model-based method is analyzed by the inherent kinematic properties, without considering interactions between catheter and atrium model. But the EP intervention is inevitable on complicated interaction with endocardial environment. In comparison, the model-free control can adapt to the interaction by updating the inverse Jacobian, especially under the circumstance of soft contact with phantom.

(b) Efficiency
The model-free control method demonstrated a remarkable reduction in the missed lesion targets (35.8%), and the maximum number of continuous missed lesion target spheres (46.2%), both of which correspond to a low p value (≤ 0.05). For the total travel distance of the catheter tip during the task, the model-free method demonstrated a slight disadvantage (-7.65%). This phenomenon indicates that the model-free method could provide faster and more sensitive response to the operators input.

Conclusion and future work

The proposed experimental validation platform, comprising an MR Safe catheterization robot and a human–robot interface, could realize both model-based and model-free methods for catheter control. Subject test that emulates an ablation task is conducted to quantitatively evaluate the performance of both control methods. Quantitative evaluation of both methods is conducted via a subject test. Accuracy indices (e.g., mean of the closest distance between the catheter tip and the closest target during ablation) and efficiency indices (e.g., the proportion of missed lesion target) are adopted. It could be seen that model-free control method performed better than the model-based one in both aspects of accuracy (19.1% improvement in the tip-to-target ablation distance) and efficiency (35.8% reduction in the missed-target proportion and 46.2% reduction in the number of continuously missed targets).

The proposed experiment using static LA model is the first step to validate the catheter control methods, as well as its robot platform. In our future work, we intend to enhance the preclinical validation using a dynamic left atrial phantom, of which the deformation can be induced by simulated pulsatile flow of liquid. A higher number of subjects will be invited to this new simulated task.

Funding This work is supported in part by the Croucher Foundation, the Research Grants Council (RGC) of Hong Kong (17202317, 17227616 and 27209515), Aptorum Group Limited and Signate Life Sciences Limited.

Compliance with ethical standards

Conflict of interest The authors declare that they have no conflict of interest.

Table 1 Measured performance indices averaged across 10 subjects in performing the robotic catheterization of the phantom model

Model	Model-based		Model-free		Improvement	
Accuracy	Mean	STD	Mean	STD	%	*p*-val.
Mean tip-to-target distance during ablation (mm)	6.94	1.34	5.61	1.31	19.1	0.08
Mean times of ablation turning on (sec)	23.7	10.9	24.1	7.2	− 1.88	0.89
Ablation duration (sec)	1.49	0.36	1.76	0.48	− 18.7	0.07
Efficiency	Mean	STD	Mean	STD	%	*p*-val.
Mean proportion of missed targets (%)	51.9	14.7	33.3	11.9	35.8	0.03
Maximum number of continuously missed targets	55.1	24.1	29.7	3.16	46.2	0.01
Total travel distance (mm)	649	176	699	320	− 7.65	0.60

Ethical approval All procedures performed in studies involving human participants were in accordance with the ethical standards of the institutional and/or national research committee and with the 1964 Helsinki declaration and its later amendments or comparable ethical standards.

Informed consent Informed consent was obtained from all individual participants included in the study. This article does not contain patient data.

References

1. Feng Y, Guo Z, Dong Z, Zhou XY, Kwok KW, Ernst S, Lee SL (2017) An efficient cardiac mapping strategy for radiofrequency catheter ablation with active learning. Int J Comput Assist Radiol Surg 12(7):1199–1207
2. Josephson M (2008) Clinical cardiac electrophysiology. Wolters Kluwer Health/Lippincott Williams & Wilkins, Philadelphia
3. Rafii-Tari H, Payne CJ, Yang GZ (2014) Current and emerging robot-assisted endovascular catheterization technologies: a review. Ann Biomed Eng 42(4):697–715
4. Wongcharoen W, Tsao HM, Wu MH, Tai CT, Chang SL, Lin YJ, Lo LW, Chen YJ, Sheu MH, Chang CY, Chen SA (2006) Morphologic characteristics of the left atrial appendage, roof, and septum: implications for the ablation of atrial fibrillation. J Cardiovasc Electrophysiol 17(9):951–956
5. Lardo AC, McVeigh ER, Jumrussirikul P, Berger RD, Calkins H, Lima J, Halperin HR (2000) Visualization and temporal/spatial characterization of cardiac radiofrequency ablation lesions using magnetic resonance imaging. Circulation 102(6):698–705
6. Raval AN, Karmarkar PV, Guttman MA, Ozturk C, DeSilva R, Aviles RJ, Wright VJ, Schenke WH, Atalar E, McVeigh ER, Lederman RJ (2006) Real time MRI guided atrial septal puncture and balloon septostomy in swine. Catheter Cardiovasc Interv 67(4):637–643
7. Razavi R, Hill DLG, Keevil SF, Miquel ME, Muthurangu V, Hegde S, Rhode K, Barnett M, Vaals JV, Hawkes DJ, Baker E (2003) Cardiac catheterisation guided by MRI in children and adults with congenital heart disease. Lancet 362(9399):1877–1882
8. Lee KH, Fu KC, Dong Z , Leong MCW, Cheung CL, Lee APW, Luk W , Kwok KW (2018) MR-safe robotic platform for MRI-guided intra-cardiac catheterization. IEEE ASME Trans Mechatron https://doi.org/10.1109/TMECH.2018.2801787
9. Kwok KW, Lee KH, Chen Y, Wang W, Hu Y, Chow GCT, Zhang HS, Stevenson WG, Kwong RY, Luk W, Schmidt EJ, Tse Z (2014) Interfacing fast multi-phase cardiac image registration with MRI-based catheter tracking for MRI-guided electrophysiological ablative procedures. Circulation 130:A18568
10. Bock M, Muller S, Zuehlsdorff S, Speier P, Fink C, Hallscheidt P, Umathum R, Semmler W (2006) Active catheter tracking using parallel MRI and real time image reconstruction. Magn Reson Med 55(6):1454–1459
11. Kwok KW, Chen Y, Chau TCP, Luk W, Nilsson K, Schmidt E, Tse Z (2014) MRI-based visual and haptic catheter feedback: simulating a novel system's contribution to efficient and safe MRI-guided cardiac electrophysiology procedures. J Cardiovasc Magn Reson 16(1):O50
12. Webster RJ III, Jones BA (2010) Design and kinematic modeling of constant curvature continuum robots: a review. Int J Robot Res 29(13):1661–1683
13. Ganji Y, Janabi-Sharifi F (2009) Catheter kinematics for intracardiac navigation. IEEE Trans Biomed Eng 56(3):621–632
14. Ganji Y, Janabi-Sharifi F (2007) Kinematic characterization of a cardiac ablation catheter. In: 2007 IEEE/RSJ international conference on intelligent robots and systems (IROS), pp 1876–1881
15. Liu T, Cavusoglu MC (2014) Three dimensional modeling of an MRI actuated steerable catheter system. In: 2014 IEEE international conference on robotics and automation (ICRA), pp 4393–4398
16. Greigarn T, Cavusoglu MC (2014) Task-space motion planning of MRI-actuated catheters for catheter ablation of atrial fibrillation. In: 2014 IEEE/RSJ international conference on intelligent robots and systems (IROS), pp 3476–3482
17. Back J, Lindenroth L, Rhode K, Liu H (2017) Model-free position control for cardiac ablation catheter steering using electromagnetic position tracking and tension feedback. Front Robot AI 4:17
18. Yip MC, Camarillo DB (2016) Model-less hybrid position/force control: a minimalist approach for continuum manipulators in unknown, constrained environments. IEEE Robot Autom Lett 1(2):844–851
19. Yip MC, Camarillo DB (2014) Model-less feedback control of continuum manipulators in constrained environments. IEEE Trans Robot 30(4):880–889
20. Kern MJ, Sorajja P, Lim MJ (2015) Cardiac catheterization handbook. Elsevier, Amsterdam, pp 273–286
21. Wang W, Dumoulin CL, Viswanathan AN, Tse Z, Mehrtash A, Loew W, Norton I, Tokuda J, Seethamraju RT, Kapur T, Damato AL, Cormack RA, Schmidt EJ (2015) Real time active MR tracking of metallic stylets in MR guided radiation therapy. Magn Reson Med 73(5):1803–1811
22. Hoyle RH (1999) Statistical strategies for small sample research. Sage, Thousand Oaks, p 33